Antarctic Science 5 (3): 297–307 (1993)

Association of dolerite and lamprophyre dykes, Jetty Peninsula (Prince Charles Mountains, East Antarctica)

EUGENE V. MIKHALSKY[1] and JOHN W. SHERATON[2]

[1] 190121 St. Petersburg, Maklina 1, VNIIOkeangeologia, Russia
[2] Australian Geological Survey Organisation, P.O. Box 378, Canberra, ACT 2601, Australia

Abstract: A compositionally varied swarm of mafic dykes in the Jetty Peninsula area was emplaced about 320 Ma ago (K-Ar age). There are three major groups: Group 1 dykes range from transitional-alkaline dolerites to camptonites, Group 2 are trachydolerites, and Group 3 are diorite to quartz diorite porphyries. Group 1 dykes have very similar ratios of most incompatible elements and were derived from the same (or a very similar) enriched lithospheric mantle source region ($\in_{Nd}$ -0.18 to -3.05) with high Nb and Ta (i.e., OIB, ocean island basalt, characteristics). However, the presence of several distinct subgroups with different incompatible element abundances implies significantly different degrees of melting. Group 2 trachydolerites are much more fractionated (*mg* 22–36), but were apparently derived from a similar, although somewhat more enriched ($\in_{Nd}$ -2.26 to -4.63) source. Group 3 diorites are compositionally quite distinct and may have been derived by intracrustal melting. Enrichment of the mantle source(s) of Groups 1 and 2 dykes apparently occurred about the same time as high-grade metamorphism in the area, and may have been coeval with crust formation in nearby parts of Gondwana.

Received 30 March 1990, accepted 4 November 1992

Key words: Mafic dykes, geochemistry, mantle enrichment, Prince Charles Mountains

Introduction

The northern Prince Charles Mountains (PCM) are part of a granulite-facies mobile belt which is composed mostly of Late Proterozoic high-grade metamorphic rocks (felsic orthogneisses with lenses and small bodies of mafic and ultramafic granulites, pelitic gneisses and calc-silicate gneisses) metamorphosed and deformed about 1000 Ma ago (Tingey 1982, Kamenev 1991, Thost & Hensen 1992). Manifestations of Phanerozoic rifting concentrated in this area are Permian coal-bearing sedimentary rocks in the Beaver Lake graben, Mesozoic alkaline-ultramafic stocks and sills, and rare early Cenozoic alkaline basalt flows.

Mafic dykes have been recognized in many ice-free areas of East Antarctica and locally form dense swarms (Sheraton *et al.* 1987). Their composition ranges from tholeiitic to alkaline. Most tholeiitic dykes are of Proterozoic age and crop out in Archaean cratonic blocks or, less commonly, Middle Proterozoic metamorphic terranes (Sheraton *et al.* 1990). Alkaline dykes are commonly, but not exclusively, Phanerozoic (Sheraton, 1983). Rare, thin, unmetamorphosed mafic dykes are widespread throughout the northern PCM and have varied chemical compositions; most are only slightly alkaline to transitional, even tholeiitic, but lamprophyres are also present (Mikhalsky, unpublished data). In the Beaver Lake area these dykes are particularly common and form a N–S trending swarm on Jetty Peninsula (Fig. 1). The petrography and chemical composition of these dyke rocks are similar to "olivine basalt" and "alkali olivine basalt" described by Sheraton (1983) elsewhere in the northern PCM and Mawson Coast.

On Jetty Peninsula, mafic dykes cut metamorphic rocks of the crystalline basement, but are not known to intrude the Permian coal-bearing strata. The exposed land surface represents a Late Cretaceous peneplain (Kolobov 1980) that is strongly affected by physical weathering. Thus, good exposures are rare and only a few exhibit clear dyke intersections. The dykes strike predominantly in a northerly direction (355–010°), but range between NW (310°) and NE (030°). They have thin chilled margins, dip to the west at 40–50°, and are commonly 0.5–1.5 m thick, although a few attain 5–8 m. They have sharp straight contacts which commonly exhibit cataclastic structures and quartz veinlets. Three dyke emplacement events were recognized in the field. Field evidence includes rare dyke intersections, and relationships with a fault zone and associated quartz veins which predate some dykes but postdate others.

The oldest (Group 1) dykes are the most numerous. They comprise transitional (rarely tholeiitic) to alkaline dolerites and camptonites. The latter exhibit most of the petrographical and geochemical criteria proposed by Rock (1977, 1987) for the alkaline lamprophyres, although modal feldspathoid is lacking. Nevertheless, the name camptonite is used here because feldspathoid abundance is not considered to be a critical factor and many Russian authors, following Zavaritsky's (1955) scheme, do not preclude the possibility of such lamprophyres being feldspathoid-free. However, these rocks might equally well be classified with a group of volatile-poor lamprophyres using terms like "camptonitic basalt" (Rock 1987). The camptonites contain rare small lherzolite nodules of deep-seated origin.

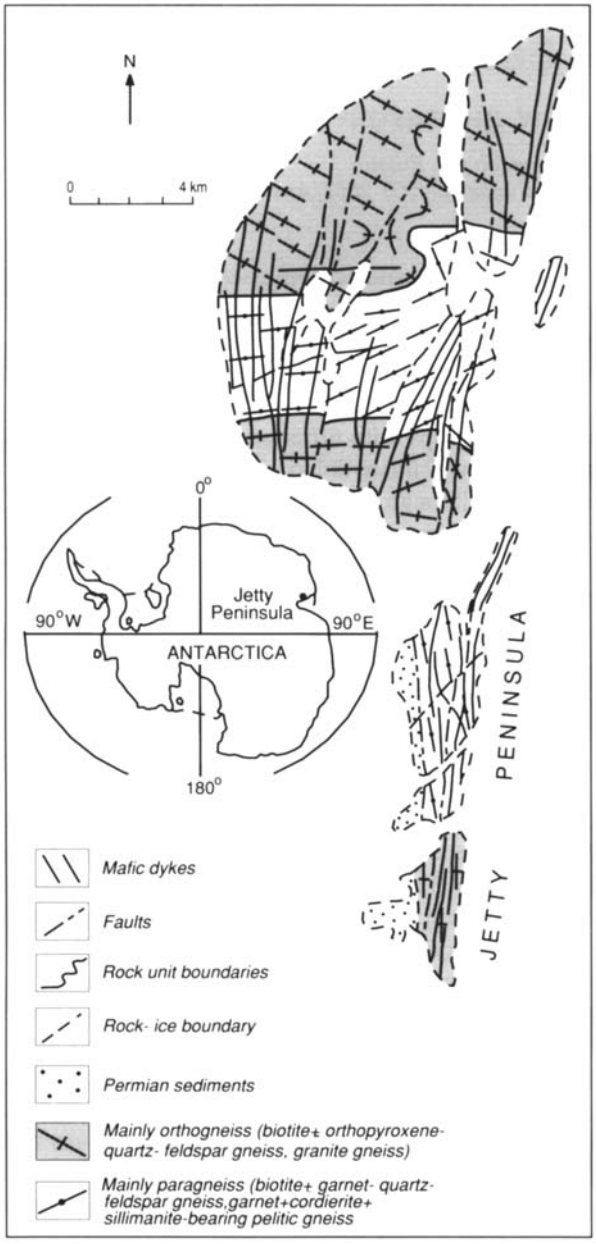

Fig. 1. Geological sketch map of Jetty Peninsula.

The younger (Group 2) dykes are rare and consist of trachydolerites with chemical compositions corresponding with those of the mugearites and benmoreites of East Africa (Wilson 1989). They could be classified as monzodiorites (after Streckeisen 1976), but the name trachydolerite is used here following the Soviet classification (Anonymous 1981), in which monzonite is used for more intermediate and calc-alkaline rocks.

The youngest dykes (Group 3) are represented by a few compositionally distinct diorite porphyries. The age of mafic dykes from this area has been measured at 310 Ma by the K-Ar method (Hofmann 1991). A new set of data obtained from other rock samples collected by the author from the same dyke swarm (Groups 1 and 2) and analysed by Prof. J. Hofmann is presented in Table I. A combined set of data in Fig. 2 yields a 321 ± 10 Ma reference line. All the main rock types described below follow this pseudoisochron, although the very high MSWD value (47) suggests some K and Ar mobility.

Petrography

The three dyke groups differ from each other in mineralogy, texture and chemical composition, with much smaller variations within each group. Group 1 and 2 dykes can be subdivided further on the basis of textural and/or mineralogical criteria, which correlate with geochemical variations. Most rocks are nearly fresh, but some are strongly altered with chlorite, carbonate, leucoxene, saussurite, opacite and epidote being the most common secondary minerals. Such altered dykes occur adjacent to shear and mylonitic zones or quartz veins, and therefore the alteration is thought to be related to younger tectonic events and hydrothermal activity. Other secondary minerals, including uralitic amphibole, albite, fine-grained biotite, and serpentine, represent deuteric (autometamorphic) alteration. They are dispersed throughout the dykes but rarely comprise more than 15%.

Representative microprobe analyses are listed in Table II. The data were obtained at "Mechanobr" laboratory (St.Petersburg) using a Cambridge Instruments "CamScan-4" microprobe with a "LINK" energy-dispersive X-ray spectrometer. The analytical conditions were as follows: beam current 5 nA, counting times 50 sec, accelerating voltage 20 kV.

Group 1 rocks

The dolerites are fine- to medium-grained dark greenish-grey or grey rocks with massive or ocellar structure. The texture varies considerably, whereas the gross mineral composition remains more or less constant. Three textural varieties may be distinguished: ophitic (Subgroup 1a), intergranular (Subgroup 1b), and porphyritic (Subgroup 1c) dolerites. Small spherical ocelli are more common in porphyritic rocks and are composed of carbonate or epidote. Accessory minerals include apatite, sphene, and Fe-Ti oxides.

Table I. K-Ar analytical data.

Sample	K %	^{40}K 10^{-7} mol/g	^{40}Ar 10^{-9} mol/g	median
1 28–2	1.16±0.04	0.346±0.012	1.098±0.026 1.123±0.026	1.111±0.026
2 57–6	2.88±0.05	0.859±0.015	2.015±0.041	2.015±0.041
3 1–4	4.04±0.08	1.205±0.024	2.733±0.054 2.550±0.058	2.642±0.055

Note 1 = dolerite, 2 = camptonite, 3 = trachydolerite. Errors are 2σ.

https://doi.org/10.1017/S0954102093000392 Published online by Cambridge University Press

Ophitic dolerites consist of relatively large plagioclase laths (An_{50-60}, 35–40%), *anhedral* ophitic grains of augite ($Ca_{44}Mg_{41}Fe_{15}$, 40–45%) and some interstitial alkali feldspar ($Na_{54}K_{27}Ca_{19}$), late magmatic plagioclase (10–20%), chlorite (altered glass, 5%) and opaque minerals (up to 5%).

Intergranular dolerites consist of fine-grained interstitial *subhedral* salite ($Ca_{45}Mg_{45}Fe_{10}$ to $Ca_{47}Mg_{37}Fe_{16}$, 40–50%) between small plagioclase laths (An_{45-50}, 40–45%), primary biotite (*mg* = 51–55, where *mg* = atomic 100(Mg/(Mg+Fe)), and chloritized glass (5–15%). The rocks also contain sparse altered ferromagnesian prismatic grains, now composed of talc and minor chlorite, but which are probably pseudomorphs after olivine.

Porphyritic dolerites contain numerous (10–20%) small zoned phenocrysts (or, rather, primocrysts) of clinopyroxene (with salite or augite $Ca_{44-46}Mg_{41-46}Fe_{10-13}$ cores and Ti-augite $Ca_{50}Mg_{37}Fe_{13}$ rims) and olivine (Fo_{80-85}). Some irregular and tabular olivine grains may represent broken pieces of a restite phase. The groundmass consists of plagioclase (An_{24-60}), albite, K-feldspar, *euhedral* salite ($Ca_{48}Mg_{37}Fe_{15}$), and biotite (*mg*=38–49).

The *camptonites* (Subgroup 1d) are fine-grained black rocks with characteristic porphyritic textures and ocellar structure. Hypidiomorphic-granular or poikilitic textures are typical of the groundmass. The rocks contain clinopyroxene and olivine phenocrysts (15–40%); clinopyroxene phenocrysts are zoned from cores of endiopside ($Ca_{42}Mg_{50}Fe_{8}$) to Ti-augite rims ($Ca_{50}Mg_{37}Fe_{13}$). Olivine phenocrysts (Fo_{79-81}) are strongly resorbed. The groundmass consists of euhedral kaersutite grains (20–30%) up to 1.5 mm in length, and small

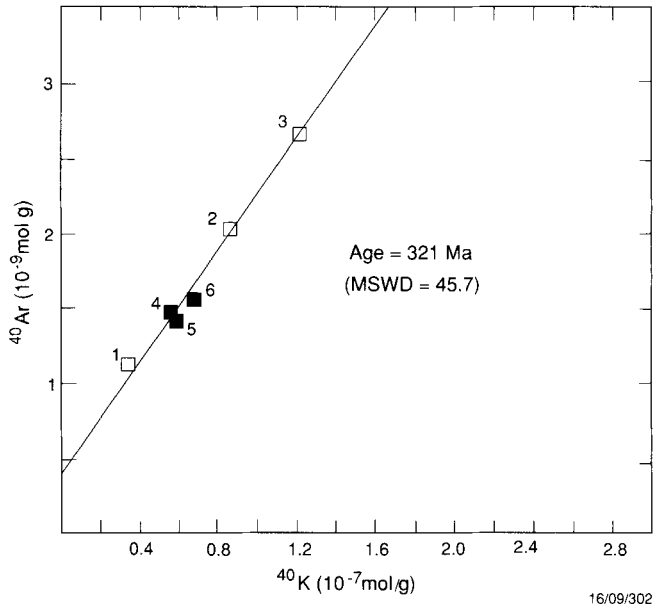

Fig. 2. K-Ar plot for new samples (□) and previously presented data by Hofmann (1991) (■). Sample numbers: 1, 4–6 = dolerites, 2 = camptonite, 3 = trachydolerite.

grains of Ti-augite ($Ca_{51}Mg_{35}Fe_{14}$, 10–15%) enclosed in relatively large plagioclase crystals (An_{50-55}, 20–30%). Minor primary biotite (*mg*=49) and alkali feldspar (up to 10 %) are present. The rocks contain carbonate ocelli (up to 5 mm) and smaller leucocratic globules which consist mainly of alkali feldspar and minor amphibole. The lack of boundary

Table II. Representative microprobe data.

Sample*	1	2	3	4	5	6	7	8
SiO	39.13	51.77	42.61	50.33	49.79	38.48	37.78	39.08
TiO		1.10	3.70	0.89	1.31	5.44	7.24	2.12
Al_2O_3		4.71	9.67	4.25	5.95	16.72	14.68	12.34
Cr_2O_3		0.02		0.47				2.41
Fe_2O_3	1.57	0.01		4.49	3.48			0.59
FeO	14.29	6.21	8.76	1.17	5.79	14.27	12.11	26.47
MnO	0.32	0.13	0.34	0.45		0.20		0.42
NiO		0.10						
MgO	44.69	15.80	11.91	16.98	15.30	9.37	10.42	3.25
CaO		20.42	21.97	20.33	16.59	12.32	11.85	10.53
Na_2O			1.04	0.65	1.79	1.22	2.35	3.24
K_2O						11.96	1.66	1.96
Ca		44	50	42	37			
Mg		43	37	50	47			
Fe		13	13	8	16			
mg	85					54	62	18
CANA						1.8	2.0	2.0
NAB						0.00	0.12	0.24

*1 = olivine (from porphyritic dolerite), 2-5 = clinopyroxenes: 2 = porphyritic dolerite phenocryst core, 3 =rim, 4 = camptonite phenocryst; 5 = trachydolerite phenocryst; 6, 7 = kaersutites from camptonite, 8 = amphibole from trachydolerite. *mg*- atomic $100(Mg/(Mg+Fe^{2+}))$, CANA- $(Ca+Na)_B$, NAB- Na_B (following IMA classification, Leake, 1978).

https://doi.org/10.1017/S0954102093000392 Published online by Cambridge University Press

Table III. Representative chemical analyses.

Sample	10–10	4/6.2	24–3	51–5	57–6	6–1	9–1	19–4	1–4	2013+
Group/ subgroup	1a	1b	1b	1c	1d	1d	2a	2b	2c	3
SiO_2	45.66	46.76	45.27	45.65	45.69	45.65	48.65	50.79	53.29	62.60
TiO_2	2.02	2.22	2.22	2.29	2.33	2.26	2.06	1.91	1.21	1.18
Al_2O_3	14.62	16.12	14.16	14.94	15.00	14.94	17.57	16.93	17.55	14.40
Fe_2O_3	3.85	2.50	2.70	2.83	3.38	2.21	2.20	1.97	2.14	2.53
FeO	8.61	8.42	8.41	7.06	6.70	8.17	8.07	8.21	7.20	5.15
MnO	0.15	0.15	0.14	0.14	0.15	0.14	0.16	0.15	0.18	0.10
MgO	7.35	7.47	8.35	7.13	6.49	7.47	2.75	2.45	1.36	1.49
CaO	9.84	7.19	8.66	7.53	7.65	8.95	5.45	4.66	3.75	1.60
Na_2O	2.59	3.57	3.10	3.16	2.96	3.11	4.24	3.95	4.95	3.16
K_2O	1.11	1.03	1.87	3.45	3.88	2.92	3.83	4.14	5.10	3.72
P_2O_5	0.37	0.53	0.51	0.71	0.73	0.63	1.14	0.98	0.71	0.54
LOI	3.66	3.88	4.48	5.04	4.98	3.43	3.82	3.77	2.51	2.71
rest	0.45	0.48	0.46	0.52	0.52	0.54	0.52	0.56	0.44	
total	100.28	100.32	100.33	100.45	100.46	100.42	100.46	100.47	100.39	99.18
					C.I.P.W. norms					
Q	-	-	-	-	-	-	-	-	-	23.34
C	-	-	-	-	-	-	-	-	-	3.56
Or	6.56	6.09	11.05	20.39	22.93	17.26	22.63	24.46	30.14	21.98
Ab	21.76	30.21	17.98	13.82	11.86	11.73	28.21	33.42	32.55	26.75
An	24.99	24.92	19.20	16.39	16.18	18.18	17.60	16.24	10.61	4.41
Ne	0.08	-	4.47	7.00	7.14	7.90	4.15	-	5.06	-
Di	17.56	5.94	16.61	13.27	13.86	17.98	1.68	0.40	2.89	-
Hy	-	2.52	-	-	-	-	-	1.60	-	9.31
Ol	17.41	18.17	17.95	15.56	14.31	15.12	12.81	11.66	9.99	-
Mt	2.92	2.58	2.62	2.32	2.35	2.46	2.43	2.41	2.21	3.68
Il	3.84	4.22	4.22	4.35	4.42	4.29	3.91	3.63	2.30	2.25
Ap	0.88	1.26	1.21	1.68	1.73	1.49	2.70	2.32	1.68	1.28

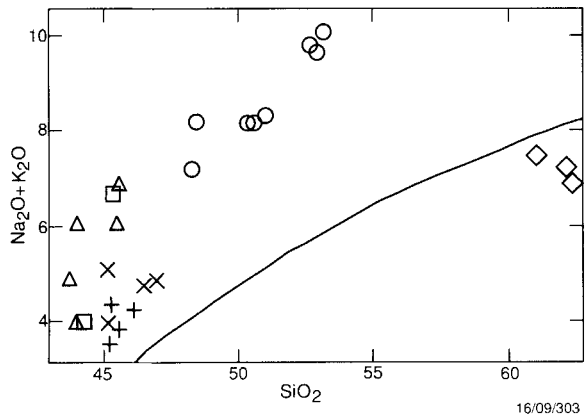

Fig. 3. Alkalis vs SiO_2 plot. + = ophitic dolerites (Subgroup 1a), × = intergranular dolerites (Subgroup 1b), □ = porphyritic dolerites (Subgroup 1c), Δ = camptonites (Subgroup 1d), ○ = trachydolerites (Group 2). ◇ = diorite porphyries (Group 3). Heavy line = alkaline (upper)-subalkaline field divider (after Irvine & Baragar 1971).

nucleation and the similarity in chemical composition of amphiboles from both rock groundmass and globules suggest that the leucocratic ocelli represent droplets of an immiscible liquid phase.

Group 2 rocks

The trachydolerites are fine-grained light greenish-grey rocks with rare carbonate ocelli, and phenocrysts of augite (Ca_{37} Mg_{47} Fe_{16}) and/or plagioclase (An_{45-50}). Textures are porphyritic, hypidiomorphic-granular or subophitic. The groundmass consists of plagioclase (An_{35-40} cores; albitic An_{5-15} rims), alkali feldspar (anorthoclase) and ferromagnesian minerals. Albite seems to be of late igneous, rather than of metasomatic origin. Feldspars compose 70–85% of the rocks, their relative proportions varying widely. Three rock types can be distinguished according to their ferromagnesian mineral assemblages: pyroxene-biotite (Subgroup 2a), biotite (Subgroup 2b) and amphibole-bearing (Subgroup 2c) trachydolerites. The ferromagnesian minerals include anhedral salite (Ca_{48} Mg_{31} Fe_{21}, 0–10%), subhedral biotite (mg=24, 5–25%) and ferropargasite (0–20%). Low

https://doi.org/10.1017/S0954102093000392 Published online by Cambridge University Press

Table III. continued

Sample	10–10	4/6.2	24–3	51–5	57–6	6–1	9–1	19–4	1–4	2013+
Group/ subgroup	1a	1b	1b	1c	1d	1d	2a	2b	2c	3
					Trace elements in parts per million					
Ba	455	727	689	1149	1199	1065	1697	1790	1359	1600
Rb	45	51	53	94	104	80	88	88	104	nd
Sr	491	513	563	832	786	778	1077	785	642	570
Pb	3	5	4	6	6	5	10	16	15	nd
Th	<2	4	2	4	4	5	10	12	15	nd
U	<0.5	0.5	<0.5	1.0	1.0	0.5	1.0	1.5	2.0	nd
Zr	143	183	182	254	258	237	274	309	363	275
Nb	32	51	51	81	84	73	100	94	126	nd
Y	22	24	22	24	24	24	32	36	38	23
La	27	33	31	52	53	49	76	79	85	nd
Ce	50	75	63	96	99	92	128	150	154	nd
Nd	23	37	30	40	44	40	55	58	59	nd
Pr	6	9	8	11	10	7	12	16	15	nd
Sc	27	25	22	19	19	24	12	14	10	9
V	228	193	190	148	151	189	76	84	8	39
Cr	189	286	317	306	386	416	72	259	80	18
Ni	141	144	203	173	179	158	16	15	14	36
Cu	95	77	70	50	50	64	27	18	19	nd
Zn	130	91	105	87	92	103	104	95	104	nd
Ga	20	20	19	18	20	21	20	21	22	7
As	1.0	8.5	1.0	<0.5	<0.5	1.5	2.0	2.0	1.5	nd
S	1700	1500	1200	900	800	1100	600	800	500	nd
Hf	5	6	7	10	9	8	9	12	11	nd
Ta	<2	3	7	7	5	<2	5	5	8	nd
Yb	2.4	2.1	nd	nd	2.2	2.4	nd	2.0	1.9	nd
mg	56.07	59.48	61.76	60.88	58.28	60.65	36.45	33.97	23.81	29.63
Ba/Y	21.0	30.3	31.3	47.9	50.0	44.0	53.0	49.7	35.8	69.6
Ba/Zr	3.2	4.0	3.8	4.5	4.6	4.5	6.2	5.8	3.7	5.8
P/Zr	11.3	12.6	12.2	12.2	12.3	11.6	18.2	13.8	8.5	43.0
Ti/Zr	84.7	72.7	84.7	54.0	54.1	57.2	45.1	37.1	20.0	25.7
Ce/Zr	0.35	0.41	0.35	0.38	0.38	0.39	0.47	0.49	0.42	nd
Zr/Nb	4.47	3.59	3.57	3.14	3.07	3.25	2.74	3.29	2.88	nd
Zr/Y	6.50	7.63	8.27	10.58	10.75	9.88	8.56	8.58	9.55	11.96
Rb/Sr	0.092	0.099	0.094	0.113	0.132	0.103	0.082	0.112	0.162	nd
K/Ba	20.2	11.8	22.5	24.9	26.9	22.8	18.7	19.2	31.1	19.3
K/Rb	205	168	293	305	310	303	361	391	407	nd
K/Nb	288	168	304	354	383	332	318	366	336	nd
Sr/Zr	3.43	2.80	3.09	3.28	3.05	3.28	3.93	2.54	1.77	2.09
Y/Nb	0.69	0.47	0.43	0.30	0.29	0.33	0.32	0.38	0.30	nd

Data were obtained by XRF method at AGSO. + Trace element abundances determined by thermo-emission method, major elements by wet chemistry.
mg = atomic 100 Mg/(Mg + 0.85 Fe_{total}) used for C.I.P.W. norm calculations.

mg-numbers suggest that most biotite is of secondary origin. In amphibole-bearing rocks the amphibole occurs as euhedral crystals up to 1 mm across; these have high alkali feldspar contents (up to 60%). Accessories include magnetite and Ti-magnetite (1–5%), apatite, and sphene.

Group 3 rocks

The diorite porphyries are medium-grained light-grey rocks with porphyritic textures. Large plagioclase phenocrysts are strongly altered to sericite and form up to 20% of the rock. The groundmass consists of plagioclase laths (An_{30-35}, 50–60%), anhedral biotite (10–20%), hornblende (5%), K-feldspar (5%) and quartz (2–3%). Secondary albite (10–15%) is also present. More evolved dykes contain more quartz (up to 20%).

https://doi.org/10.1017/S0954102093000392 Published online by Cambridge University Press

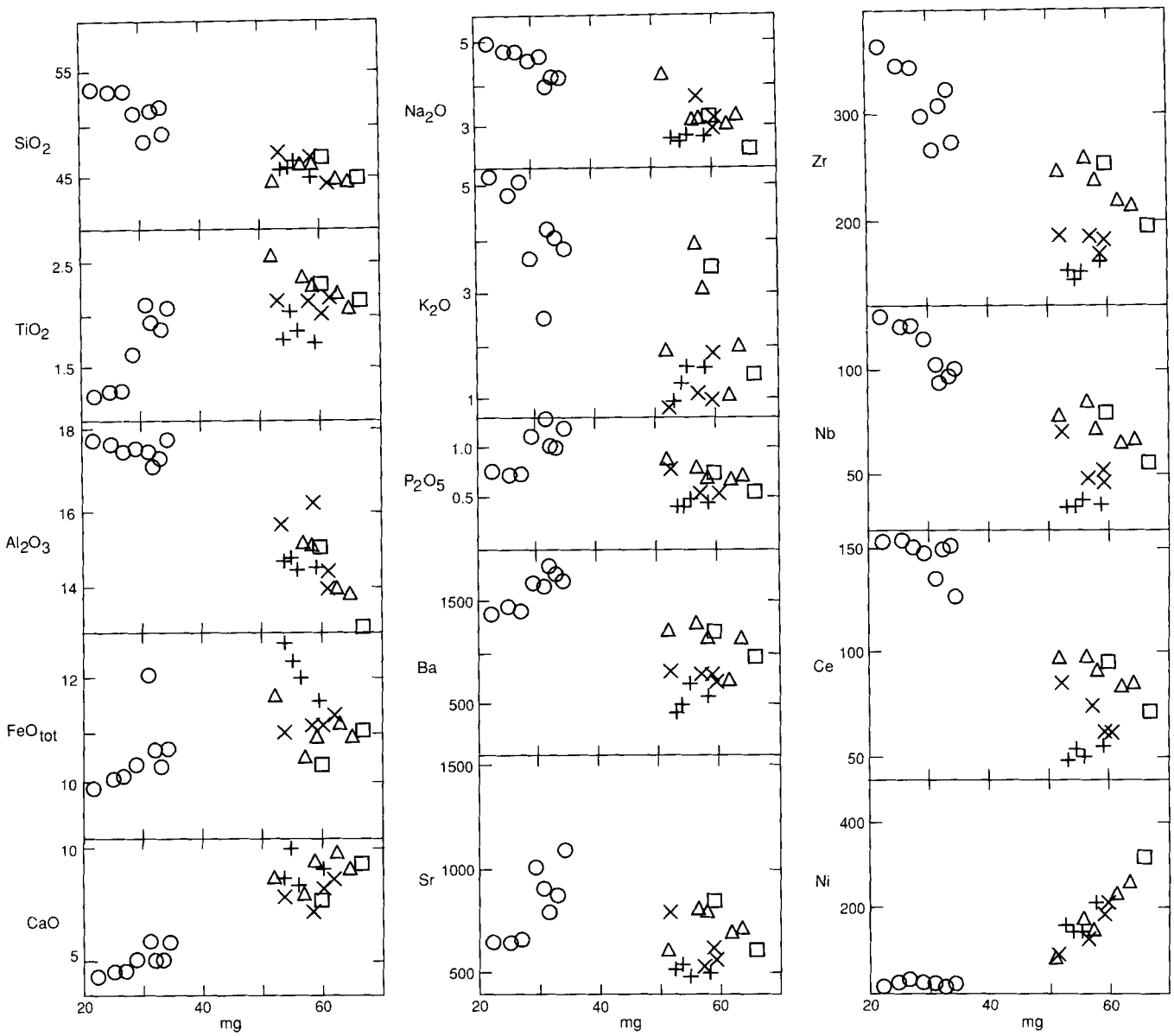

Fig. 4. *mg*-number vs selected major and trace element plots. Symbols as in Fig. 3.

Geochemistry

Forty-two samples of the dyke rocks were analysed by wet chemistry for major oxides, and twenty-four of these for a range of major and trace elements and major elements by XRF methods (Norrish & Hutton 1969, Norrish & Chappell 1977) in the laboratory of the Australian Geological Survey Organisation. In addition Yb was determined by a thermo-emission method at "Sevsapgeologia" (St.Petersburg) for some samples. Representative analyses are given in Table III. Although most of the samples analysed for trace elements do not show extensive secondary alteration, chemical changes during alteration cannot be discounted. Rock samples collected from a single dyke show minor chemical variations. Most major and some trace elements abundances differ by factors of 1.05–1.20, whereas Ni, Cr, K, Rb, Sr and, Ba vary by factors of up to 1.35; V, Cu, Zn and As also show significant variations. The consistent compositional differences between subgroups, and systematic variation trends for many elements (Figs 4 & 5) suggest that most of the chemical variations are due to magmatic rather than post-magmatic processes, and that chemical changes during alteration were probably minor. Rocks of Subgroups 1c & d (especially camptonites) contain alkali feldspar-rich globules, and variations in K, Rb, Ba and Sr abundances are likely to reflect different ocellus contents in the analysed rocks. The only ocellus-free camptonite sample from a dyke margin has relatively low K, Ba and Rb contents, whereas other major and trace element abundances are essentially constant. Variations of Cr and Ni abundances may reflect olivine and/or clinopyroxene fractionation.

https://doi.org/10.1017/S0954102093000392 Published online by Cambridge University Press

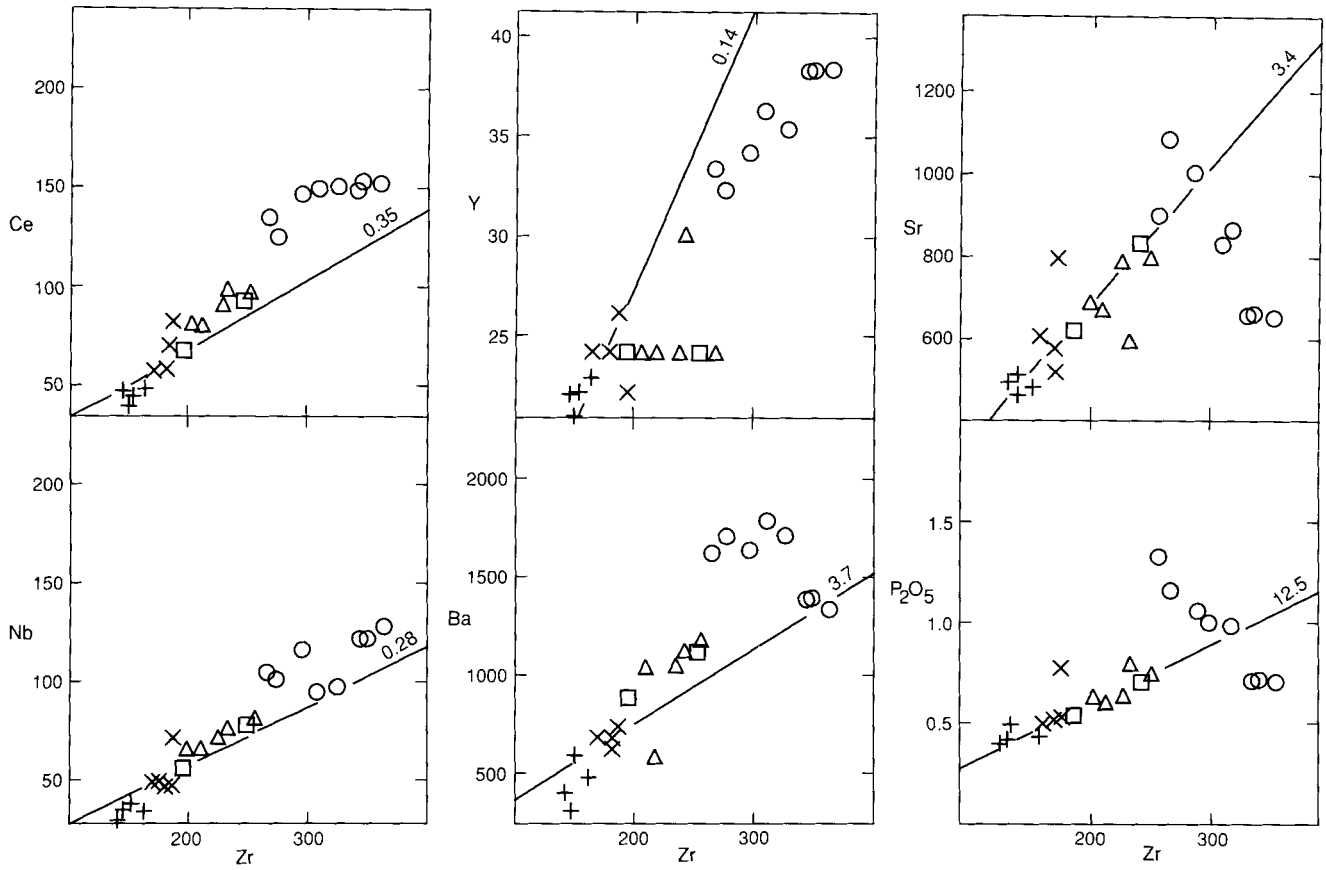

Fig. 5. Zr vs selected trace element plots. Symbols as in Fig. 3. Reference lines have constant element/Zr ratios, which are indicated.

Different dyke types within Group 1 have similar gross chemical compositions but distinctly different abundances of many trace elements, particularly Ba, Rb, Zr, Nb, Hf, Ta and LREE (light rare-earth elements). All Group 1 dykes are strongly enriched in LREE, LILE (large-ion lithophile elements) and HFSE (high field-strength elements) compared to Middle Proterozoic tholeiitic dykes in the Vestfold Block (Collerson & Sheraton 1986), with Subgroup 1a showing the least enrichment, and Subgroup 1d (camptonites) the most. Group 1 rocks have relatively high Rb/Sr (0.08–0.12) and low Y/Nb (0.30–0.75), Zr/Nb (3.1–4.5), K/Nb (168–356), K/Rb (150–310), and K/Ba (12–27) ratios.

Dykes of Subgroups 1a & b are Q-saturated to slightly Q-undersaturated whereas the rocks of Groups 1c & d are Q-undersaturated with up to 11% of normative nepheline. All the rocks are alkaline in terms of an alkalies *v.* SiO_2 plot (Fig.3), although the lack of, or only low, normative Ne in Subgroups 1a & b suggests that, following Ringwood (1975), these rocks can be classified as transitional dolerites. Subgroups 1c & d are more enriched in alkalies for a given SiO_2 content; they show rather a large range of *mg*-numbers (*mg* = atomic 100 (Mg/(Mg + 0.85 Fe_{total})) between 53–67, which overlaps with that of Subgroups 1a & b (55–62). Together with their relatively low Ni (100–330 ppm) and Cr (170–400 ppm) abundances, this suggests that the melts were not primitive. Although there are few clear correlations between *mg* number and major and trace element abundances for the Group 1 rocks as a whole, individual Subgroups show reasonably good correlations for many elements. For example, Subgroups 1c & d show negative correlations between *mg* number and P_2O_5, TiO_2, Na_2O, Zr, Nb, LREE, Ba and Sr and positive correlations with Ni and Cr (Fig. 4).

Subgroups 1a & b are relatively enriched in many incompatible elements (e.g. Zr), but have similar SiO_2 contents to Subgroups 1c & d. Hence, different degrees of partial melting were probably important in determining the incompatible element abundances. Thus camptonites and porphyritic dolerites are likely to represent the lowest degrees of partial melting, and ophitic dolerites the highest. Most Group 1 rocks exhibit near-constant ratios on incompatible element/Zr plots (Fig.5), with many other incompatible element ratios (K/Nb, K/Ba, P/Ce, Rb/Sr, K/Rb) also being virtually constant, suggesting that the different subgroups originated from the same or very similar mantle source regions. By contrast, Ti/Zr, Ce/Y, and Zr/Y ratios of Subgroups 1a & b and 1c & d are significantly different, implying that Y and Ti were more compatible and suggesting pyroxene ± garnet ± Fe-Ti control. Smaller variations in incompatible

https://doi.org/10.1017/S0954102093000392 Published online by Cambridge University Press

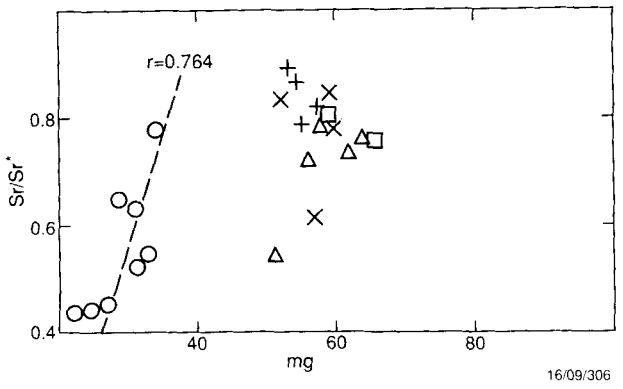

Fig. 6. *mg*-number vs Sr/Sr* plot. Symbols as in Fig. 3. Sr/Sr* is the normalized Sr abundance divided by the interpolated value derived by averaging the normalized Ce and Nd abundances. The dashed line approximates the regression.

element ratios could be due to source heterogeneity, crustal contamination, and/or significant differences in the proportions of residual minerals (possibly including minor phases) which would be more important for relatively low percentage, transitional to alkaline melts. The range of Subgroup 1c & d compositions, in particular, could be due largely to crystal fractionation of both Mg-rich and Al-rich phases within the cotectic assemblage. The lack of correlation between *mg* number and Sr/Sr* ratio (Fig.6), and near-constant Zr/Sr ratio preclude significant plagioclase fractionation (except for two of the more evolved samples). Hence, amphibole (kaersutite) + olivine + clinopyroxene fractionation is more likely to have taken place. Mass balance calculations made using the 1985 D.G. Gerst, B.H. Baker and A.R. McBirney "GPP" geochemical programme package, confirm that fractionation of these assemblages can explain much of the compositional variations for Subgroups 1c & d (Table IV). Unfortunately, distribution coefficient data for kaersutite in alkaline melts are lacking, so that calculations of trace-element fractionation are subject to large uncertainties.

A preliminary Sm-Nd study of Group 1 rocks reveals a wide scatter of data far exceeding analytical uncertainties with $\in_{Nd}$(T) (calculated for T = 321 Ma) ranging between -0.18 and -3.05 (Table V), and decreasing with increasing Ba, Th, Nb, La, Ce, Sr and Zr abundances. These features may reflect either source heterogeneity or different degrees of crustal involvement.

Spidergram patterns (Fig.7) show considerable enrichment of all incompatible elements, with different subgroups being essentially similar. The spidergrams have relatively smooth slopes without prominent troughs or peaks apart from Th anomalies on the OIT-normalized plot. Hence, melt contamination by upper crustal material is unlikely to have been of major importance because such a process would probably have induced marked Ti, P, Sr, Nb and Ta troughs.

The chemical compositions of Group 2 rocks vary widely.

Table IV. Mass balance calculations.

Mix	1 parent 1	daughter 1 rock calcul.		2 daughter 2 rock calcul.		3 parent 2	daughter calcul.
SiO_2	47.26	47.37	47.87	52.34	52.20	51.09	51.96
TiO_2	2.24	2.43	2.37	1.99	1.32	2.23	2.00
Al_2O_3	13.82	16.20	16.05	18.16	18.30	17.87	18.03
FeO*	11.04	10.56	11.11	10.03	10.19	9.32	9.89
MnO	0.16	0.16	0.17	0.18	0.21	0.17	0.20
MgO	10.87	7.65	7.48	2.99	3.01	4.50	3.02
CaO	9.46	8.55	8.51	5.01	5.18	6.21	5.03
Na_2O	2.63	3.48	3.29	4.42	4.34	4.38	4.67
K_2O	2.00	2.90	2.44	3.88	3.85	3.23	3.92
P_2O_5	0.55	0.72	0.71	1.01	1.42	1.00	1.27

Mix 1: Parent 1 – (0.064.Ol + 0.108.Px_1 + 0.051.$Amph_1$) = daughter 1; r = 0.853.
Mix 2: Parent 1 – (0.083.Ol + 0.234.Px_1 + 0.259.$Amph_1$ + 0.038.Pl) = daughter 2; r = 0.733.
Mix 3: Parent 2 – (0.019.Ol + 0.026.Px_2 + 0.081.$Amph_2$ + 0.087.Pl) = daughter 2; r = 0.319.
Parent 1 - the most primitive subgroup 1 c rock (porphyritic dolerite), daughter 1– average of 6 more evolved dolerites and camptonites, daughter 2 –average of 10 trachydolerites (Subgroup 2b), parent 2– average of 3 less evolved trachydolerites (Subgroup 2a). Mineral compositions used are listed in Table II: 1–Ol, 2-Px_1, 5-Px_2, 6-$Amph_1$, 7-$Amph_2$.

All rocks plot within the alkaline field on an alkalies *v.* SiO_2 diagram, although only some are Ne-normative (up to 5%) while others are slightly Hy-normative. Group 2 rocks are highly evolved, with low *mg*-numbers (22 to 36), Ni, and Cr. FeO_{tot}, TiO_2, CaO, P_2O_5, Ba, Sr and Sr/Sr* are positively correlated with *mg* number, whereas SiO_2, Na_2O, K_2O, Zr, Nb Ce, and Y are negatively correlated and Ni and Cr poorly correlated (Figs 4 & 6). These features could be consistent with AFC processes (De Paolo 1981) with major plagioclase control. However, mass balance calculations show that more evolved varieties (Subgroup 2b) can only be derived from less evolved (Subgroup 2a) melts by fractional crystallization of Ol+Px+Amph+Pl, which is inconsistent with the observed phenocryst assemblages. Similar results are produced using the most primitive rock composition of Subgroup 1c as a parent (Table IV), although, in this case, the same fractionating assemblage (with different Px and Amph compositions) may be more plausible. Subgroup 2c compositions cannot be related to more primitive rocks by any feasible fractional crystallization process. Hence, the various Subgroups (2a–c) probably crystallized from distinct parent magmas.

Many incompatible element ratios of Subgroups 2a and 2b (K/Nb, K/Ba, P/Ce, Rb/Sr, Zr/Nb, Zr/Y) are generally similar to those of Group 1, whereas K/Rb, Ce/Y, and Ba/Zr ratios are consistently higher and Ti/Zr lower. Subgroup 2c dykes show even more divergent ratios with, for example, low Ba/Zr, P/Zr and Sr/Zr. Many of these differences could have been caused by more extensive plagioclase, clinopyroxene, apatite, and Ti-magnetite fractionation, and variations in Ce/Y probably

reflect variations in the amount of residual clinopyroxene (or garnet). However, some degree of source heterogeneity may be required to explain, for example, the high Ba/Zr and P/Zr of Subgroup 2a, the latter suggesting variable apatite in the source region.

Spidergram patterns for individual samples are broadly similar both to each other and to Group 1 rocks, suggesting a generally similar mantle source. Depletions in Ti, and to lesser extents, Sr probably reflect Ti-magnetite and plagioclase fractionation, respectively. Subgroup 2c rocks are the most enriched in the more incompatible elements (Rb-Ta), but are relatively depleted in most elements from Sr to Y, particularly Sr, P and Ti, features consistent with extensive fractional crystallization. Regular spidergram patterns militate against crustal contamination having been of major importance, as granulites are commonly depleted in Rb, Th, Nb, Ta, and, in some case, Y (Wilson 1989).

Group 2 rocks show a similar range of Sm-Nd compositions to Group 1 rocks (Table V). $\in_{Nd}(T)$ varies between -2.26 and -4.63, decreasing with increasing LREE, Th, Zr, Nd, and Rb and decreasing Sr and Ba. Until the isotope characteristics of granulite-facies metamorphic rocks of the northern PCM are better studied, their possible influence on the composition of the igneous rocks will remain obscure. However, the relatively small range of $\in_{Nd}$ is unlikely to reflect significant crustal contamination.

Group 3 rocks (diorite and quartz diorite porphyries) are more evolved (*mg*= 11–30). Their relatively high Ni contents and normative Q and C (Table III) indicate that they cannot be related to Groups 1 or 2 through crystal fractionation processes, and they were clearly derived from a distinct (possibly crustal) source region. Different Ba/Y, P/Zr, Ti/Zr, Zr/Y ratios are consistent with this suggestion.

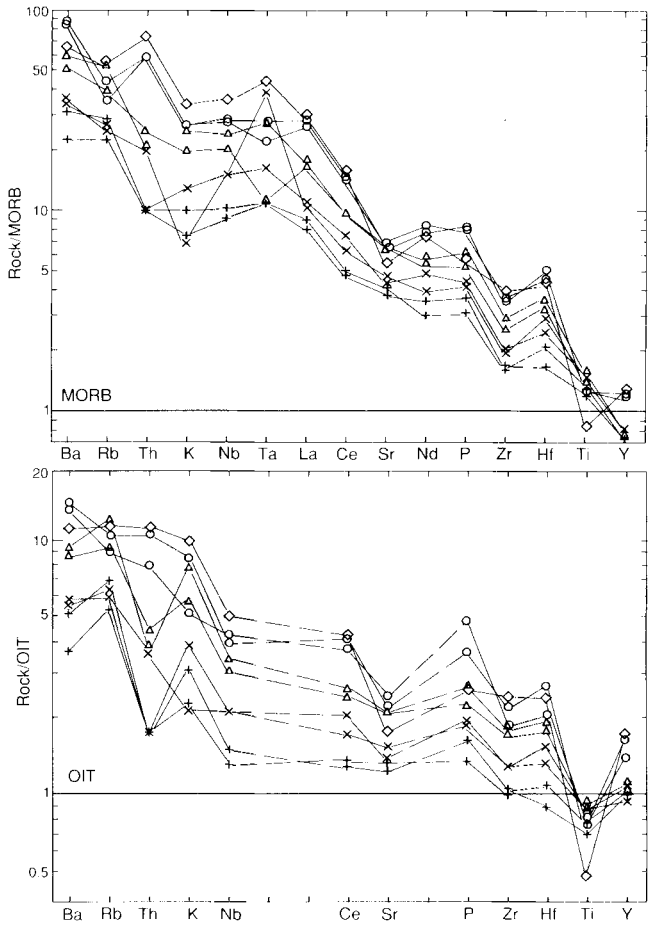

Fig. 7. Spidergrams for representative Group 1 and Group 2 rocks. **a.** MORB-normalized (normalization factors from Thompson et al. 1984); **b.** OIT-normalized (normalization factors from Wilson 1989). Symbols as in Fig. 3, except diamonds = Subgroup 2c trachydolerite.

Conclusions

All Group 1 and 2 dykes were apparently derived from very similar enriched mantle source regions, although systematic variations in bulk composition and incompatible element abundances imply significant differences in degrees of melting, and possibly some source heterogeneity. They thus form a genetically related, but not comagmatic, suite.

Both Groups show marked enrichment in most incompatible elements (LILE, LREE, and HFSE) compared to MORB (with the exception of Y) and, to lesser extents, OIT (Fig.7). The OIT-normalized spidergrams show the most mobile LILE (K, Rb, Ba, and Th) to be enriched by factors of 2–5 in rocks with larger degrees of partial melting (Subgroup 1a) whereas enrichment in other elements is relatively small (up to 2 times OIT). The source of the Jetty Peninsula dyke rocks is thus likely to have been an enriched mantle reservoir. The positive correlations of Sr with Rb and Ba for Group 1 dykes are more consistent with mantle enrichment (and/or partial melting processes) than crustal contamination. Group 2 melts may have undergone minor crustal contamination or may have been derived from a more enriched source. However, very low La/Nb ratios (0.6–0.7 for Group 1 rocks and 0.7–0.85 for Group 2 rocks) are unlikely to be due to contamination (Thompson *et al.*1984). Like the low La/Nb, relatively high Th/Yb and Ta/Yb ratios suggest a within-plate environment (Pearce 1982). Such compositional features could be explained in terms of magma derivation from a Nb-rich OIB (ocean-island basalt)-like component, or involvement of a Nb-rich eclogite component. Thus high LILE and LREE abundances are likely to reflect the involvement of an enriched lithospheric mantle reservoir. Relatively smooth spidergram patterns, with no significant negative anomalies, do not argue for major contamination, although some degree of contamination cannot be discounted.

Group 1 rock types were probably derived from a common source region by different degrees of partial melting, with camptonites representing the lowest and ophitic dolerites the highest degrees. Group 1 rocks differ from each other in:

https://doi.org/10.1017/S0954102093000392 Published online by Cambridge University Press

Table V. Sm-Nd isotope data.

Sample	Subgroup	Nd ppm	Sm ppm	$^{147}Sm/^{144}Nd$	$^{143}Nd/^{144}Nd$	Nd_t	$f_{Sm/Nd}$	$\varepsilon_{Nd}(T)$	T_{DM}
10–10	1a	23.96	5.026	0.12680	0.512480±7	0.512214	-0.36	-0.18	1060
24–3	1b	32.66	6.94	0.12836	0.512376±9	0.512106	-0.35	-2.28	1240
40–2	1b	39.85	6.87	0.10419	0.512352±6	0.512133	-0.47	-1.76	1023
57–6	1c	43.07	7.79	0.10935	0.512297±8	0.512067	-0.44	-3.05	1141
9–1	2a	54.26	9.38	0.10446	0.512326±7	0.512107	-0.47	-2.26	1058
5/8–1	2b	56.41	9.78	0.10485	0.512318±5	0.512098	-0.47	-2.44	1072
19–4	2b	58.86	12.72	0.13125	0.512262±9	0.511986	-0.33	-4.63	1463
1–4	2c	60.27	10.27	0.10303	0.512211±10	0.511995	-0.48	-4.45	1189

Note. Constants used: ^{147}Sm decay $6.54.10^{-12}$ 1/yr; $^{147}Sm/^{144}Nd_{CHUR}=0.1967$; $^{143}Nd/^{144}Nd_{CHUR}=0.512636$; $^{147}Sm/^{144}Nd_{DM} = 0.225$; $^{143}Nd/^{144}Nd_{DM} = 0.513163$
Data obtained at the Institute of Precambrian Geology and Geochronology (St. Petersburg).

1) textural features, expressed by pyroxene-grain morphology (euhedral-anhedral) and pyroxene-plagioclase phase relations,

2) abundance of phenocrysts,

3) distribution and composition of ocelli, and

4) contents of LILE and HFSE, and $\in_{Nd}$ values.

Many of these features might have been dependent on different fluid activities during initial melting and/or melt evolution during ascent of magma through the crust. More rapid ascent of volatile-rich camptonite magma probably prevented ferromagnesian phenocrysts from resorption while slower ascent of volatile-poor magma led to their common resorption. The presence of small alkaline ocelli in camptonites indicates formation of an immiscible liquid, which may have been facilitated by high fluid activity. Camptonites, together with the transitional to alkaline dolerites, seem to form a compositionally coherent suite. With *mg*-numbers < 65 and Ni and Cr abundances not exceeding 330 and 400 ppm, respectively, none of these rocks apparently represents a primitive melt. However, it is possible that melting of unusually enriched mantle, rather than four-phase lherzolite, could produce such low-*mg* partial melts. If so, the compositional variations of the porphyritic dolerites and camptonites (Subgroups 1c and 1d) could be due to different degrees of partial melting, rather than fractionation of olivine, clinopyroxene and amphibole. Some enrichment of the source region (e.g. in LILE), possibly due to a metasomatising volatile flux penetrating the lithosphere (Bailey 1987), may have occurred during magma generation, but isotopic data suggest that mantle enrichment was much earlier (see below).

Most Group 2 dykes could have been derived by fractionation of olivine, clinopyroxene, amphibole and plagioclase, probably with apatite and Ti-magnetite joining them at a later stage, from a Group 1-type parent melt. However, melting of a slightly different (more enriched) source region, with somewhat higher Ba/Zr, Th/Zr, Ce/Zr, and P/Zr than those of Group 1 is possible. Subgroup 2c was probably derived by even more extensive fractionation of magma from the same (or a similar) source. Group 3 dykes have calc-alkaline affinities and probably represent the evolved products of distinct parent melts, formed either by melting in the lower crust due to heating by a mantle-derived magma chamber, or by fractionation of such a magma.

If crustal assimilation was not important, the range of $\in_{Nd}$ must reflect varying degrees of mantle LREE enrichment. T_{DM} model ages are mostly 1050–1200 Ma, although these are likely to represent upper limits for the time of mantle enrichment event(s). They are, in fact, only slightly older than the age of high-grade metamorphism over an extensive area covering PCM, Princess Elizabeth Land and adjacent regions (Tingey 1982). The Late Proterozoic, between 1100 and 800 Ma, is thought to have been a time of new crust formation in some parts of East Antarctica (Yoshida 1992), although the few model ages available for northern PCM crust are older (1630–1980 Ma, S-S Sun personal communication 1992, Hensen *et al.* 1992). Model ages for the Jetty Peninsula dyke rocks are thus consistent with the suggestion that crust-forming and mantle-enrichment events occurred in the Late Proterozoic. A mantle-enrichment event also seems to have been roughly co-eval with felsic crust formation in the Bunger Hills, where 500 ma alkaline mafic dykes were derived from long-term enriched mantle (T_{DM} ages = 2080–2290 Ma) (Sheraton *et al.* 1990). Jurassic Karoo picritic basalts of Zimbabwe were apparently formed by melting of lithospheric mantle which underwent Sm-Nd fractionation about 1050 Ma ago, also a time of crust formation in adjacent parts of Gondwana (Ellam & Cox 1989).

The alkaline mafic dyke swarm marks a N–S trending fracture zone forming the structure of the Lambert Glacier graben. Both graben development and dyke swarm emplacement are believed to represent an initial stage of Lambert rift graben formation in the Carboniferous.

Acknowledgements

The authors are grateful to Professor J. Hofmann for K-Ar

analyses, to Dr B. Beliatsky for Sm-Nd data, to Dr S-S Sun for fruitful discussions, and to Drs T. Alabaster and J. Smellie for reviewing an early version of the manuscript. G. Michelowski drafted the figures. JWS publishes with the permission of the Director, AGSO.

References

ANONYMOUS. 1981 *Klassifikatsia i nomenclatura magmaticheskih gornyh porod*, [Classification and nomenclature of igneous rocks]. Moscow: "Nedra" Publishing Office, 160 pp.

BAILEY, D.K. 1987. Mantle metasomatism - perspective and prospect. *In* FITTON J.G. & UPTON B.G.J. *eds, Alkaline igneous rocks*. Special Publication of the Geological Society of London, No. 30, 1-12.

COLLERSON, K.D. & SHERATON, J.W. 1986. Age and geochemical characteristics of a mafic dyke swarm in the Archaean Vestfold Block, Antarctica: inferences about Proterozoic dyke emplacement in Gondwana. *Journal of Petrology*, **27**, 853-886.

DE PAOLO, D.J. 1981. Trace element and isotopic effects of combined wallrock assimilation and fractional crystallization. *Earth and Planetary Science Letters*, **53**, 189-202.

ELLAM, R.M. & COX, K.G. 1989. A Proterozoic lithospheric source for Karoo magmatism: evidence from the Nuantesi picrites. *Earth and Planetary Science Letters*, **92**, 207-218.

HENSEN, B., MUNSKARD, N. & THOST, D.E. 1992. Geochemistry and geochronology of Proterozoic granulites from the northern Prince Charles Mountains, East Antarctica. *ANARE Research Notes*, No. 85, 9.

HOFMANN, J. 1991. Fault tectonics and magmatic ages in the Jetty Oasis area, Mac. Robertson Land: a contribution to the Lambert rift development. *In* THOMSON, M.R.A., CRAME, J.A. & THOMSON, J.W. *eds, Geological evolution of Antarctica*. Cambridge: Cambridge University Press, 107-112.

IRVINE, T.N. & BARAGAR, W.R.A. 1971. A guide to the chemical classification of the common volcanic rocks. *Canadian Journal of Earth Sciences*, **8**, 523-548.

KAMENEV, E.N. 1991. Structure and evolution of Precambrian cratons and metamorphic belts in East Antarctica. *Volume of abstracts, Sixth International symposium on Antarctic Earth Sciences*. Tokyo: National Institute of Polar Research, 261-262.

KOLOBOV, D.D. 1980. Relief i oledenenie iuzhnyh gor Prince Charles [Relief and glaciation of the southern Prince Charles Mountains]. The Antarctic. *Soviet Committee of Antarctic Research Reports*, **19**, 146-151.

LEAKE, B.E. 1978. Nomenclature of amphiboles. *Mineralogical Magazine*, **42**, 533-563.

NORRISH, K. & CHAPPELL, B.W. 1977. X-ray fluorescence spectrometry. *In* ZUSSMAN, J. *ed. Physical methods in determinative mineralogy*. London: Academic Press, 201-272.

NORRISH, K & HUTTON, J.T. 1969. An accurate X-ray spectrographic method for the analysis of a wide range of geological samples. *Geochimica and Cosmochimica Acta*, **33**, 431-453.

PEARCE, J.A. 1982. Trace element characteristics of lavas from destructive plate boundaries. *In* THORPE R.S. *ed. Andesites: orogenic andesites and related rocks*. Chichester: Wiley, 525-548.

RINGWOOD, A.E. 1975. *Composition and petrology of the Earth's mantle*. New York, N.Y.: McGraw-Hill, 618 pp.

ROCK, N.M.S. 1977. The nature and origin of lamprophyres: some definitions, distinctions and derivations. *Earth-Science Reviews*, **13**, 123-169.

ROCK, N.M.S. 1987. The nature and origin of lamprophyres: an overview. *In* FITTON J.G. & UPTON B.G.J. *eds. Alkaline igneous rocks*. Special Publication of the Geological Society of London, No. 30, 191-226.

SHERATON, J.W. 1983. Geochemistry of mafic igneous rocks of the northern Prince Charles Mountains, Antarctica. *Journal of the Geological Society of Australia*, **30**, 295-304.

SHERATON, J.W., THOMSON, J.W. & COLLERSON, K.D. 1987. Mafic dyke swarms of Antarctica. *In* HALLS, H.C. & FAHRIG, W.F. *eds, Mafic dyke swarms*. Geological Association of Canada Special Paper, No 34, 419-432.

SHERATON, J.W., BLACK, L.P MCCULLOCH, M.T.& OLIVER, R.L. 1990. Age and origin of a compositionally varied mafic dyke swarm in the Bunger Hills, East Antarctica. *Chemical Geology*, **85**, 215-246.

STRECKEISEN, A. 1976. To each plutonic rock its proper name. *Earth Science Reviews*, **12**, 1-33.

THOMPSON, R.N., MORRISON, M.A., HENDRY, G.L. & PARRY, S.J. 1984. An assessment of the relative roles of a crust and mantle in magma genesis: an elemental approach. *Philosophical Transactions of the Royal Society of London*, **A310**, 549-590.

THOST, D.E. & HENSEN, B.J. 1992. Structure and petrology of granulite facies gneisses of the Porthos Range, northern Prince Charles Mountains, Antarctica. *ANARE Research Notes*, No. 85, 19.

TINGEY, R.J. 1982. The geologic evolution of the Prince Charles Mountains - an Antarctic Archean cratonic block. *In* CRADDOCK C. *ed. Antarctic geoscience*. Madison: The University of Wisconsin Press, 455-464.

WILSON, M. 1989. *Igneous petrogenesis*. London: Unwin Hyman, 466 pp.

YOSHIDA, M. 1992. Precambrian tectonothermal events in East Gondwanian crustal fragments and their correlation (IGCP-288). *In Japan Contribution to the IGCP*, 51-62.

ZAVARITSKY, A.N. 1955. *Izverzhennyie gornye porody* [Igneous rocks]. Moscow: AN SSSR, 479 pp.